

Synthesis, radiolabeling, and in vivo evaluation of an ^{18}F -labeled isatin analog for imaging caspase-3 activation in apoptosis

Dong Zhou, Wenhua Chu, Justin Rothfuss, Chenbo Zeng,
Jinbin Xu, Lynne Jones, Michael J. Welch and Robert H. Mach*

*Division of Radiological Sciences, Washington University School of Medicine, 510 South Kingshighway Boulevard,
St. Louis, MO 63110, USA*

Received 13 June 2006; revised 12 July 2006; accepted 13 July 2006
Available online 7 August 2006

Abstract—A non-peptide-based isatin sulfonamide analog, **WC-II-89**, was synthesized and its inhibition toward recombinant human caspase-3 and other caspases was determined. This compound showed high potency for inhibiting caspase-3 and -7, and high selectivity against caspases-1, -6, and -8. [^{18}F]**WC-II-89** was synthesized via a nucleophilic substitution of the corresponding mesylate precursor in high yield and radiochemical purity. Biodistribution studies using [^{18}F]**WC-II-89** revealed higher uptake in liver and spleen of cycloheximide-treated rats, an animal model of apoptosis, relative to control animals. Western blot analysis confirmed the presence of activated caspase-3 in the liver and spleen of cycloheximide-treated animals. MicroPET imaging studies revealed a high uptake of the radiotracer in the liver of a cycloheximide-treated rat relative to the untreated control. These data suggest that [^{18}F]**WC-II-89** is a potential radiotracer for imaging caspase-3 activation in tissues undergoing apoptosis.
© 2006 Elsevier Ltd. All rights reserved.

Apoptosis, or programmed cell death, is critical for the normal development and function of multicellular organisms as a common and universal mechanism of cell death.¹ It is a conserved process that is mediated by the activation of a series of cysteine aspartyl-specific proteases termed caspases. The abnormal regulation of cellular death via apoptosis is believed to play a key role in a variety of human diseases, such as ischemia-reperfusion injury (stroke and myocardial infarction), cardiomyopathy, neurodegeneration (Alzheimer's Disease, Parkinson's Disease, Huntington's Disease, and ALS), sepsis, Type I diabetes, fulminant liver disease, and allograft rejection.^{2,3} In addition, the beneficial effect of many drugs, especially antitumor drugs, can be attributed to their activation of the apoptotic process.^{4–9} Therefore, the development of a non-invasive imaging procedure that can study the process of apoptosis in a variety of disease states, and monitor the ability of a drug to either induce or halt apoptosis, would be of tremendous value to the research and clinical community.

Positron emission tomography (PET) and single photon emission computed tomography (SPECT) are

in vivo imaging techniques that measure the change in tissue and cellular function at the molecular level. The agents used so far for imaging apoptosis in vivo are mostly based on Annexin V,¹⁰ which is a 36-kDa protein that binds selectively with high affinity to externalized phosphatidylserine. Phosphatidylserine is normally found only on the interior of the cell membrane but translocates to the exterior of the cell membrane in the early stages of apoptosis. However, since the externalization of phosphatidylserine also occurs in necrosis, a further step, the propidium iodide exclusion test,¹¹ is required to discriminate between apoptosis and necrosis in vitro. Although this test is routinely used to distinguish apoptosis from necrosis using ex vivo techniques such as flow cytometry, it cannot be applied to in vivo techniques such as PET and SPECT. In addition, the slow clearance of radiolabeled Annexin V from blood generally requires imaging studies be conducted 4–6 h after administration of the radiotracer. Although this long time interval between radiotracer injection and image acquisition is compatible with the radionuclides used in SPECT imaging studies, it is not suitable for the short half-life radionuclides used in PET.

An alternative strategy for measuring and imaging cells and tissues undergoing apoptosis is the use of antibodies

Keywords: Caspase-3; Apoptosis; Positron emission tomography.

* Corresponding author. Tel.: +1 3143628538; fax: +1 3143620039;
e-mail: rhmach@mir.wustl.edu

directed toward enzymes that are intrinsic to the biochemical pathways of apoptosis. The enzymes responsible for the regulation and execution of apoptosis are the caspases, which exist as inactive zymogens (pro-caspases) in the cytosol and become activated when cells receive an apoptotic signal. Caspases activated early in the process of apoptosis are known as initiator caspases; the function of the initiator caspases is to activate the executioner caspases, which are responsible for the proteolytic cleavage of proteins that are necessary for cellular function. The initiator caspases are caspases-6, -8, and -9, and the executioner caspases are caspase-3 and -7. Cellular apoptosis can be initiated via two different pathways, extrinsic and intrinsic.¹¹ Since the intrinsic and extrinsic pathways involve the activation of caspase-3, immunohistochemical staining for activated caspase-3 provides an unambiguous method for measuring and imaging apoptosis. Furthermore, small molecule inhibitors of caspase-3 that can be radiolabeled with either carbon-11 ($t_{1/2} = 20.4$ min) or fluorine-18 ($t_{1/2} = 110$ min) have the potential for imaging apoptosis with PET under a variety of pathological conditions. This imaging procedure also has the capability to image chemotherapy-induced apoptosis and capacity to provide an imaging-based procedure for measuring a positive response to treatment in cancer patients.

Recently, we reported the synthesis of a number of non-peptide-based isatin sulfonamide analogs,¹² many of which displayed nanomolar potency for inhibiting caspase-3 and caspase-7, while exhibiting a low potency for inhibiting the initiator caspases, caspase-1, -6, and -8. In this letter, we describe the synthesis of a new isatin sulfonamide analog, **WC-II-89**, that is suitable for radiolabeling with fluorine-18, and the biodistribution of [¹⁸F]**WC-II-89** in an animal model of apoptosis. We also report the first microPET imaging study directly measuring caspase-3 activation in tissues undergoing apoptosis using [¹⁸F]**WC-II-89**.

The synthesis of **WC-II-89** and its precursor for ¹⁸F-labeling, **10**, is shown in the Scheme 1. *O*-Alkylation of methyl 4-hydroxybenzoate **1** was achieved by conversion to the corresponding sodium salt (sodium hydride in THF at 0 °C) followed by addition of 1-bromo-2-fluoroethane to give compound **2**, which was reduced by LiAlH₄ in ether to afford the alcohol, **3**. The hydroxyl group of **3** was then converted to the corresponding bromo analog **4** via treatment with CBr₄ and Ph₃P in CH₂Cl₂. 1-(2-Bromoethoxy)-4-(bromomethyl)benzene **6** was obtained by bromination of **5** with NBS in CCl₄. The *N*-Boc group of **7** was removed with TFA and the secondary amine was coupled with 5-chlorosulfonylisatin in THF using triethylamine as an acid scavenger to produce 5-(2-phenoxy-methyl-pyrrolidine-sulfonyl)-1*H*-2,3-dione, **8**. The isatin nitrogen was alkylated by treatment of **8** with sodium hydride in DMF at 0 °C followed by addition of **4** or **6** to give compounds **WC-II-89** and **9**, respectively. Compound **9** was then heated to reflux with silver methanesulfonate in acetonitrile to generate the precursor **10**.¹³

Inhibition of recombinant human caspase-3 and other caspases by **WC-II-89** was assessed using a fluorescent

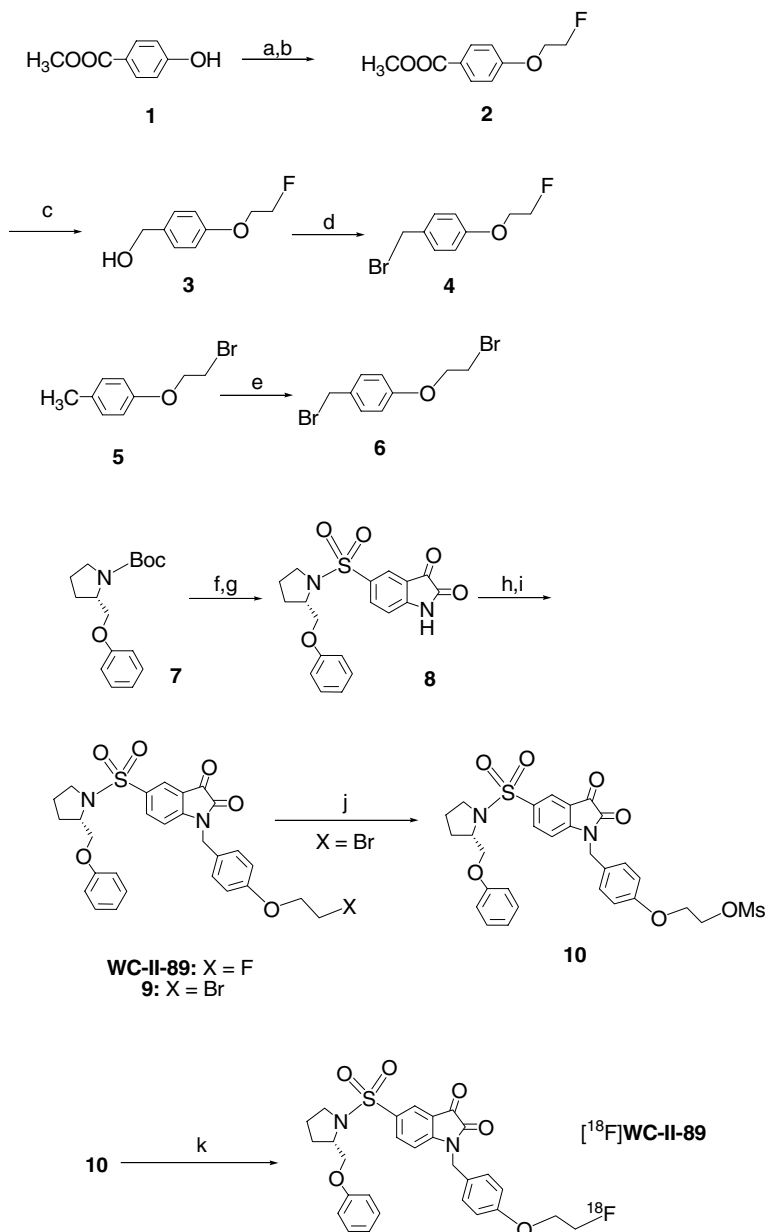
product, 7-amino-4-methylcoumarin (7-AMC), as previously reported.¹² The IC₅₀ values from the enzyme assays are shown in Table 1. **WC-II-89** shows high potency for inhibiting caspase-3 and -7, with IC₅₀ values at least 150-fold higher versus the initiator caspases-1, -6, and -8. This caspase-inhibitory profile suggests that **WC-II-89** is a potential radiotracer for imaging apoptosis with PET when labeled with fluorine-18.

Starting from **10**, the [¹⁸F]**WC-II-89** was synthesized by the nucleophilic substitution of the mesylate group with [¹⁸F]fluoride ion using the radiochemical procedure outlined in the Scheme.¹⁴ The incorporation yield was more than 70% and the synthesis time was less than 100 min. [¹⁸F]**WC-II-89** was confirmed by the co-elution with non-radioactive standard **WC-II-89** on an analytical HPLC system. The radiochemical purity of [¹⁸F]**WC-II-89** was 99% and the specific activity was determined as ~1500 mCi/μmol at the end of synthesis.¹⁵

The evaluation of [¹⁸F]**WC-II-89** as a radiotracer for imaging caspase-3 activation was determined using a well-characterized animal model of chemically induced apoptosis.^{16,17} This model, which uses the protein synthesis inhibitor, cycloheximide (CHX), was previously used in the evaluation of radiolabeled Annexin V analogs.¹⁸ Tissue morphology and TUNEL staining studies have shown that cycloheximide induces apoptosis in rat liver in both a dose-dependent and time-dependent manner. Within 3 h of treatment with 1.5, 3, or 10 mg of cycloheximide per kilogram of body weight, apoptosis was induced in rat liver.^{16,17} Therefore, we chose 3 h treatment of 5 mg/kg to induce the maximum apoptosis in rat liver, expecting a high level of caspase-3 activation.

The biodistribution results of [¹⁸F]**WC-II-89** in normal and cycloheximide-treated male Sprague–Dawley rats¹⁹ are shown in Table 2 and Figure 1. In general, the initial uptake was higher for CHX-treated rats than control rats. However, the difference between control and treated rats was reduced with time with the exception of the liver and spleen. At 1 h after injection (Fig. 1), the uptake in liver and spleen for the treated rats was 94 and 184% higher than the control animals at 1-h post-iv injection of the radiotracer. The increase in uptake of [¹⁸F]**WC-II-89** in the cycloheximide-treated versus control animals is consistent with chemically induced apoptosis and caspase-3 activation. Since the isatin analogs are competitive inhibitors of caspase-3,¹² [¹⁸F]**WC-II-89** binds to the activated form of caspase-3 in tissues undergoing apoptosis, which explains the slower wash-out of radioactivity from the liver and spleen of the cycloheximide-treated animals. The results of the biodistribution study also revealed a very low uptake of radioactivity in bone, indicating that defluorination is not a concern with this radiotracer. The result of the biodistribution study implies that [¹⁸F]**WC-II-89** is a potential PET radiotracer for imaging caspase-mediated apoptosis.

Western blot studies were carried out to measure caspase-3 levels in control and cycloheximide-treated rats²⁰



Scheme 1. Reagents: (a) NaH, THF; (b) BrCH₂CH₂F; (c) LiAlH₄, ethyl ether; (d) CBr₄, Ph₃P, CH₂Cl₂; (e) NBS, CCl₄; (f) TFA, CH₂Cl₂; (g) 5-sulfonylisatin Chloride, Et₃N; (h) NaH, DMF; (i) **4** or **6**; (j) AgOMs, acetonitrile; (k) [¹⁸F]KF, kryptofix[2.2.2].

Table 1. Inhibition of **WC-II-89** for caspases-1, -3, -6, -7, and -8

IC ₅₀ (nM)				
Caspase-1	Caspase-3	Caspase-6	Caspase-7	Caspase-8
>50,000	9.7 ± 1.3	3700 ± 390	23.5 ± 3.5	> 50,000

in order to correlate caspase-3 activity to the biodistribution results. Western blot analysis of spleen, liver, and fat for both control and treated rats is shown in Figure 2. The level of cleaved caspase-3 in the spleen and liver of the treated rats is much higher than that of the control animals, which is consistent with cycloheximide-induced apoptosis. There was no cleaved caspase-3 in the Western blot of the fat tissues from both control and treated rats. The results of the Western blot

studies correlate very well to the biodistribution data of liver, spleen, and fat at 1-h post-iv injection of the radiotracer as shown in Figure 1. The good correlation between caspase-3 activity and biodistribution of [¹⁸F]WC-II-89 in the cycloheximide-treated rats establishes the basis for imaging apoptosis using [¹⁸F]WC-II-89.

The microPET images of the liver region at 10–60 min post-iv injection of [¹⁸F]WC-II-89 are shown in Figure 3.²¹ The animal receiving a 3 h pre-treatment of cycloheximide displayed a higher uptake of [¹⁸F]WC-II-89 in the liver versus the control animal. Figure 4 shows the tissue–time activity curves from the microPET imaging study. Although the early imaging frames (0–3 min) suggest there is approximately a 20% increase in blood

Table 2. Biodistribution of [¹⁸F]WC-II-89 in normal and cycloheximide-treated (5 mg/kg, 3 h pre-treated) male Sprague–Dawley rats (200–250 g)^a

		5 min	1 h		2 h	
Blood	Control	2.70 ± 0.21	0.112 ± 0.010		0.063 ± 0.007	
	Treated	3.66 ± 0.40	0.165 ± 0.012	***	0.074 ± 0.004	ns
Lung	Control	1.42 ± 0.34	0.178 ± 0.032		0.081 ± 0.012	
	Treated	2.08 ± 0.23	0.229 ± 0.026	*	0.115 ± 0.016	*
Liver	Control	3.13 ± 0.26	0.378 ± 0.059		0.156 ± 0.015	
	Treated	4.02 ± 0.45	0.733 ± 0.118	***	0.219 ± 0.026	*
Spleen	Control	1.14 ± 0.08	0.150 ± 0.048		0.058 ± 0.010	
	Treated	2.24 ± 0.41	0.427 ± 0.052	***	0.107 ± 0.026	*
Thymus	Control	0.231 ± 0.070	0.093 ± 0.012		0.043 ± 0.003	
	Treated	0.382 ± 0.104	0.123 ± 0.020	*	0.063 ± 0.007	*
Kidney	Control	1.245 ± 0.136	0.534 ± 0.073		0.178 ± 0.037	
	Treated	1.184 ± 0.082	0.547 ± 0.048	ns	0.230 ± 0.047	ns
Muscle	Control	0.143 ± 0.009	0.077 ± 0.008		0.033 ± 0.004	
	Treated	0.094 ± 0.000	0.104 ± 0.018	**	0.064 ± 0.002	***
Fat	Control	0.119 ± 0.022	0.149 ± 0.019		0.071 ± 0.008	
	Treated	0.087 ± 0.028	0.143 ± 0.014	ns	0.086 ± 0.014	ns
Bone	Control	0.445 ± 0.036	0.132 ± 0.018		0.154 ± 0.056	
	Treated	0.661 ± 0.059	0.116 ± 0.009	ns	0.128 ± 0.027	ns

^a Student's *t*-test, *p* > 0.05; not significant (ns); **p* < 0.05; ***p* < 0.01; ****p* < 0.001.

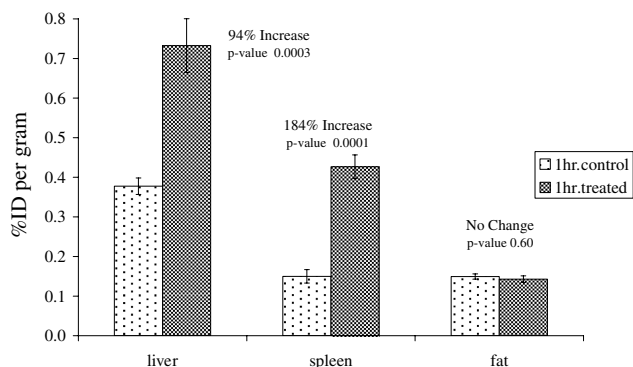


Figure 1. Selected biodistribution of [¹⁸F]WC-II-89 in control and cycloheximide (5 mg/kg) 3 h pre-treated male Sprague–Dawley rats (200–250 g). The data represent tracer uptake 1 h post-iv injection of the radiotracer.

flow to the cycloheximide-treated liver, the higher peak accumulation of [¹⁸F]WC-II-89 in the treated rat liver versus the control animal is consistent with drug-induced caspase-3 activation. The normal rat liver also displayed a faster washout of radioactivity than the cycloheximide-treated liver, which is consistent with drug-induced caspase-3 activation versus differences in

blood flow. Caspase-3 activation in the cycloheximide-treated versus control animal was also confirmed by Western blot analysis of the rat livers following completion of the microPET imaging study (data not shown). The treated:control ratios from the microPET study (Fig. 4 inset) are also identical with the 2-fold increase in uptake of [¹⁸F]WC-II-89 observed in the biodistribution study (Fig. 1).

To summarize, radiotracers for imaging apoptosis have been traditionally based on radiolabeled Annexin V, some of which have gone to clinical trials.¹⁰ Although some of these studies have been encouraging, Annexin V cannot distinguish apoptosis and necrosis in vivo since externalized-phosphatidylserine occurs in both pathways of cellular death. Therefore, there is a need to develop radiotracers that are specific for imaging cell death via apoptosis (programmed cell death) using PET.¹⁸ Since the activation of the executioner caspases, caspase-3 and -7, occurs late in apoptosis, radiolabeled inhibitors of caspase-3 and -7 represent a novel strategy for discerning programmed cell death from necrosis. A previous study reported the synthesis and carbon-11 radiolabeling of an isatin analog having a modest potency for inhibiting caspase-3.²² However, no in vivo data were reported in this meeting abstract, and the selectiv-

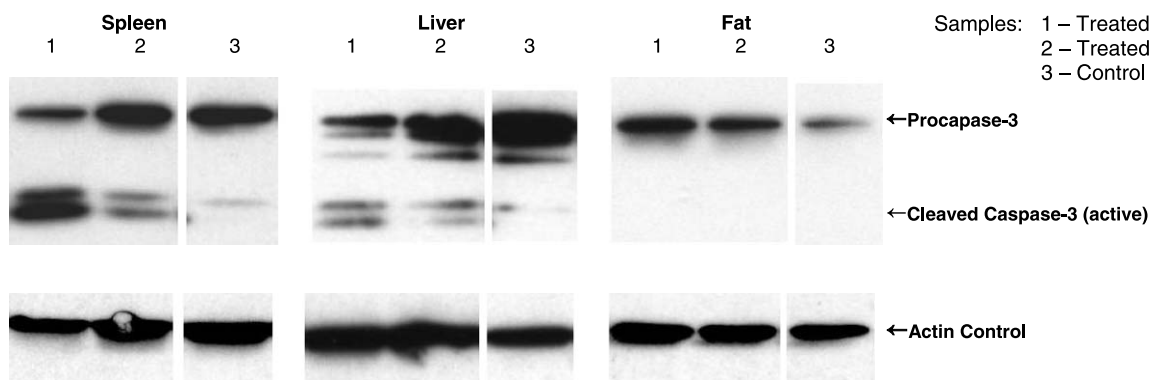


Figure 2. Western blot study of control and treated (5 mg/kg, 3 h pre-treated) male Sprague–Dawley rats (200–250 g).

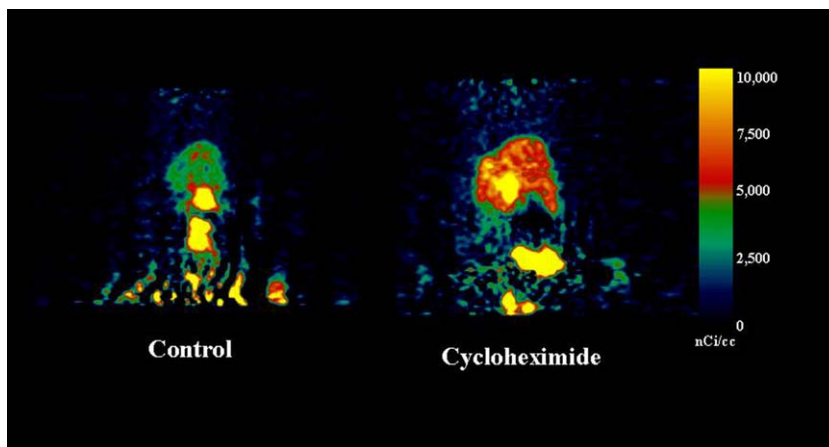


Figure 3. Whole-body MicroPET images of [^{18}F]WC-II-89 distribution in a control rat (left) and cycloheximide-treated rat (right). Images were summed from 10 to 60 min after iv injection of $\sim 150 \mu\text{Ci}$ [^{18}F]WC-II-89.

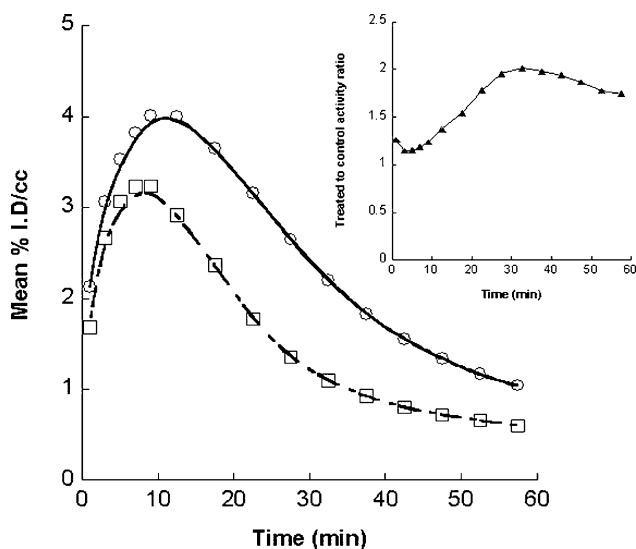


Figure 4. Tissue time-activity curves (mean percentage of injected dose per cube centimeter) of rat liver. Cycloheximide-treated rat (O); control rat (□). Inset graph shows the ratio of the liver uptake of the cycloheximide-treated versus control liver.

ity of this compound for caspase-3 versus other caspases was not mentioned. Our group previously reported the synthesis and in vitro potency of a number of isatin-based analogs having a high potency for inhibiting the executioner caspases, caspase-3 and -7, relative to caspases-1, -6, and -8.¹² In this letter, we have shown that **WC-II-89** binds to caspase-3 and -7 with high affinity and specificity versus caspases-1, -6, and -8. Biodistribution studies of [^{18}F]WC-II-89 revealed a higher uptake in the liver and spleen of rats treated with cycloheximide, a well-established murine model of chemically induced apoptosis. Western blot analysis confirmed this uptake was related to caspase-3 activation. Our results have demonstrated for the first time that apoptosis can be measured and imaged by PET using ^{18}F -labeled caspase-3 inhibitors such as [^{18}F]WC-II-89. We are currently evaluating [^{18}F]WC-II-89 in additional animal models of apoptosis.

Acknowledgments

This work was supported by HL13851, EB 001729, and CA121952. The authors thank Nicole M. Fettig, Jerrel Rutlin, and Lori Strong for animal handling and micro-PET imaging.

References and notes

- Jacobson, M. D.; Weil, M.; Raff, M. C. *Cell* **1997**, *88*, 347.
- Reed, J. C. *Nat. Rev. Drug Disc.* **2002**, *1*, 111.
- Rodriguez, I.; Matsuura, K.; Ody, C.; Nagata, S.; Vassalli, P. *J. Exp. Med.* **1996**, *184*, 2067.
- White, E. *Gene Dev.* **1996**, *10*, 1.
- Ashkenazi, A.; Dixit, V. M. *Science* **1998**, *281*, 1305.
- Evan, G.; Littlewood, T. *Science* **1998**, *281*, 1317.
- Green, D. R.; Reed, J. C. *Science* **1998**, *281*, 1309.
- Thornberry, N. A.; Lazebnik, Y. *Science* **1998**, *281*, 1312.
- Dive, C.; Hickman, J. A. *Br. J. Cancer* **1991**, *64*, 192.
- Review see Lahorte, C. M. M.; Vanderheyden, J.; Steinmetz, N.; Van De Wiele, C.; Dierckx, R. A.; Slegers, G. *Eur. J. Nucl. Med. Mol. Imaging* **2004**, *31*, 887.
- Neuss, M.; Crow, M. T.; Chesley, A.; Lakatta, E. G. *Cardiovasc. Drugs Ther.* **2001**, *15*, 507.
- Chu, W.; Zhang, J.; Zeng, C.; Rothfuss, J.; Tu, Z.; Chu, Y.; Reichert, D. E.; Welch, M. J.; Mach, R. H. *J. Med. Chem.* **2005**, *48*, 7637.
- 1-[4-(2-Fluoroethoxy)-benzyl]-5-(2-phenoxyethyl-pyrrolidine-1-sulfonyl)-1*H*-indole-2,3-dione (**WC-II-89**). A solution of **8** (97 mg, 0.25 mmol) in DMF (3 mL) was added 60% NaH (10 mg, 0.25 mmol) at 0 °C. The mixture was stirred for 5 min, then **4** (250 mg) was added. The mixture was stirred for 10 min. at 0 °C, ethyl acetate (50 mL) was added, washed with water (30 mL), NaCl (30 mL), and dried over Na_2SO_4 . After evaporation of the ethyl acetate, the crude product was purified with ether to afford 74 mg (55%) of **WC-II-89** as a yellow solid, mp 164.0–164.8 °C. ^1H NMR (300 MHz, CDCl_3) δ 8.01 (s, 1H), 7.95 (d, $J = 8.1$ Hz, 1H), 7.28–7.21 (m, 4H), 6.95–6.80 (m, 6H), 4.86 (s, 2H), 4.75 (dt, $J = 47.4$ Hz, $J = 4.2$ Hz, 2H), 4.20 (dt, $J = 28.5$ Hz, $J = 4.2$ Hz, 2H), 4.15 (m, 1H), 3.92 (m, 2H), 3.49 (m, 1H), 3.22 (m, 1H), 2.02 (m, 2H), 1.78 (m, 2H). Anal. Calcd for $\text{C}_{28}\text{H}_{27}\text{FN}_2\text{O}_6$: C, 62.44; H, 5.05; N, 5.20. Found: C, 62.50; H, 5.11; N, 5.12. 1-[4-(2-Bromoethoxy)-benzyl]-5-(2-phenoxyethyl-pyrrolidine-1-sulfonyl)-1*H*-indole-2,3-dione (**9**) was prepared according

to the same procedure for compound **WC-II-89** except using compound **6**, purified with hexane–ether (1:2) to afford 587 mg (68%) of **9** as a yellow solid, mp 164.1–164.9 °C. ¹H NMR (300 MHz, CDCl₃) δ 8.05 (s, 1H), 8.01 (dd, *J* = 8.1 Hz, *J* = 2.1 Hz, 1H), 7.32–7.25 (m, 4H), 6.70–6.84 (m, 6H), 4.91 (s, 2H), 4.32 (t, *J* = 6.0 Hz, 2H), 4.20 (m, 1H), 3.97 (m, 2H), 3.67 (t, *J* = 6.3 Hz, 2H), 3.55 (m, 1H), 3.26 (m, 1H), 2.07 (m, 2H), 1.83 (m, 2H). Anal. Calcd for C₂₈H₂₇BrN₂O₆S·0.25 H₂O: C, 55.68; H, 4.59; N, 4.64. Found: C, 55.66, 4.28; N, 4.54. Methanesulfonic acid 2-{4-[2,3-dioxo-5-(2-phenoxyethyl)-pyrrolidine-1-sulfonyl]-2,3-dihydro-1H-indol-1-ylmethyl}-phenoxy ester (**10**). A solution of **9** (300 mg, 0.5 mmol) and AgOMs (1.01 g, 5.0 mmol) in CH₃CN (10 mL) was heated to reflux overnight. After evaporation of the solvent, the crude product was purified with ether to afford 228 mg (74%) of **10** as a yellow solid, mp 151.8–152.6 °C. ¹H NMR (300 MHz, CDCl₃) δ 8.05 (s, 1H), 8.01 (dd, *J* = 8.1 Hz, *J* = 1.8 Hz, 1H), 7.33–7.25 (m, 4H), 7.00–6.84 (m, 6H), 4.90 (s, 2H), 4.60 (t, *J* = 4.8 Hz, 2H), 4.27 (t, *J* = 4.8 Hz, 2H), 4.20 (m, 1H), 3.97 (m, 2H), 3.54 (m, 1H), 3.26 (m, 1H), 3.11 (s, 3H), 2.06 (m, 2H), 1.83 (m, 2H). Anal. Calcd for C₂₉H₃₀N₂O₉S₂: C, 56.66; H, 4.92; N, 4.56. Found: C, 56.74; H, 4.88; N, 4.67.

14. Yoo, J.; Dence, C. S.; Sharp, T. L.; Katzenellenbogen, J. A.; Welch, M. J. *J. Med. Chem.* **2005**, *48*, 6366.
15. HPLC conditions for purification of [¹⁸F]**WC-II-89**: Alltech Ecosoil C18 250 × 10 mm, 10 μ; 25% acetonitrile, 45% methanol, and 30% 0.1 M ammonium formate buffer (pH 4.5); 5 mL/min, 251 nm; *t*_R = 15 min.
16. Ledda-Columbano, G. M.; Coni, P.; Faa, G.; Manenti, G.; Columbano, A. *Am. J. Pathol.* **1992**, *140*, 545.
17. Faa, G.; Ledda-Columbano, G. M.; Ambu, R.; Congiu, T.; Conti, P.; Riva, A.; Columbano, A. *Liver* **1994**, *14*, 270.
18. Yagle, K. J.; Eary, J. F.; Tait, J. T.; Grierson, J. R.; Link, J. M.; Lewellen, B.; Gibson, D. F.; Krohn, K. A. *J. Nucl. Med.* **2005**, *46*, 658.
19. All animal studies in this letter were performed in accordance with the regulations of the Washington University Institutional Animal Care and Use Committee. Mature male Sprague–Dawley rats from Charles River Laboratories were briefly anesthetized with 1–2% isoflurane in oxygen. Each rat received 10–15 μCi [¹⁸F]**WC-II-89** via the tail vein. Treated rats also received 5 mg/kg cycloheximide in saline via the tail vein three hours prior to radiotracer administration in order to induce caspase-mediated liver apoptosis. At set time-points following radiopharmaceutical injection, rats were again anesthetized and euthanized. Target and non-target organs were removed, weighed, and the radioactivity was counted using a Beckman Gamma 8000 well counter. Standard dilutions of the injected dose were counted along with the samples and uptake was calculated and reported as percent injected dose per gram (%ID/g).
20. Mature male Sprague–Dawley rats (Charles River Laboratories, Inc., Wilmington, MA) were anesthetized with 1–2% isoflurane in oxygen and treated rats were injected via tail vein with 5 mg/kg CHX/saline solution to activate caspase-mediated apoptosis. Rats were euthanized three hours post-treatment and the organs of interest were immediately snap-frozen in liquid nitrogen, then stored at –80 °C until analysis. Whole organs were homogenized in ice-cold T-PER[®] protein extraction buffer (Pierce Biotechnology, Rockford, IL) containing 5 mM DTT, 2 mM EDTA, and Complete[®] protease inhibitor cocktail tablets (Roche Diagnostics Co., Indianapolis, IN). The fully homogenized samples were then sonicated on ice, centrifuged at 4 °C at 14,000g for fifteen minutes, and the protein-containing supernatant was collected. Forty micrograms of protein from each sample was analyzed using standard immunoblotting techniques. Caspase-3 was probed with anti-caspase-3 antibody (Cell Signaling Technology, Danvers, MA) at 1:1000 dilution and horseradish peroxidase-conjugated goat anti-rabbit IgG (Cell Signaling Technology, Danvers, MA) at 1:3000. Actin was resolved using anti-β-actin antibody (Cell Signaling Technology, Danvers, MA) at 1:1000 dilution and the same secondary antibody as mentioned above. SuperSignal[®] WestDura extended duration substrate (Pierce Biotechnology, Rockford, IL) was used for detection.
21. MicroPET imaging studies were performed using a MicroPET Focus 220 and MicroPET Focus 120 scanner (Siemens/CTI, Knoxville, TN). A control and cycloheximide-treated (5 mg/kg, 3 h pre-treated) rat were anesthetized and a catheter inserted in the jugular vein. Each rat was then placed in the scanner and, following a transmission scan, was injected with ~150 μCi [¹⁸F]**WC-II-89** for a one hour dynamic imaging session. MicroPET images were reconstructed with OSEM-2D data analysis software package (Siemens/CTI, Knoxville, TN).
22. Faust, A.; Wagner, S.; Keul, P.; Schober, O.; Levkau, B.; Schaeffers, M.; Kopka, K. *J. Labelled Compd. Radiopharm.* **2005**, *48*, S260 (abstract).